

# Improving Battery Performance by Using Traffic Shaping Techniques

Carla-Fabiana Chiasserini, *Member, IEEE*, and Ramesh R. Rao, *Senior Member, IEEE*

**Abstract**—We present a new approach to minimizing of energy consumption by addressing battery management techniques that exploit the charge recovery effect inherent to many secondary storage batteries. We review results that pertain to the capacity of a battery and its dependence on the intensity of the discharge current. The phenomena of charge recovery that takes place under bursty or pulsed discharge conditions is identified as a mechanism that can be exploited to enhance the capacity of a battery. The bursty nature of many data traffic sources suggests that data transmissions may provide natural opportunities for charge recovery. We explore stochastic models to track charge recovery in conjunction with bursty discharge processes. Using the postulated model, we identify the improvement to battery capacity that results from pulsed discharge driven by bursty stochastic discharge demand. The insight from this analysis leads us to propose discharge shaping techniques that trade-off energy efficiency with delay.

**Index Terms**—Energy consumption, traffic management, wireless communications.

## I. INTRODUCTION

**P**ORTABLE DEVICES MUST often rely on battery energy to conduct communications. Display, hard disk, logic, and memory are the device components with the greatest impact on power consumption; however, when a wireless interface is added to a portable system, power consumption increases significantly. As an example, consider SmartBadge [1], a smart card that can be integrated in computing systems, mobile phones, or personal digital assistance devices; the power consumption of the RF link, display, and memory in active state is equal to 43%, 28%, and 15% of the total power consumption, respectively. In the case of a wireless local area network (WLAN) card, power consumption is equal to 1.65 W in transmission mode, equal to 1.4 W in reception mode and equal to 0.045 W in doze mode [2]. It is obvious that batteries with features such as a long lifetime, a light weight, and a small size are highly desirable in portable wireless devices. For these reasons, energy consumption management has become a critical issue in communication systems.

Various MAC protocols [3] and schemes for power management control during transmissions [4], [5] have been proposed in the literature to conserve as much energy as possible, while dynamic power management policies have been proposed in [1]

and [6]. The approach presented here differs from the previous work on energy management [1], [3]–[7] in that the goal is to understand the intrinsic behavior of batteries and then use this understanding to develop new energy efficient protocols. The goal is to increase the amount of energy that can be drained from a battery, the so-called *delivered energy*; in this way, the run-time of wireless terminals can be extended.

Typically power is drawn off a battery using a constant current discharge; however, if a pulsed current discharge is adopted, significant improvements in delivered energy seem possible [8]–[13]. In particular, the time period that elapses from when the battery is fully charged to when it is considered discharged can be significantly extended by draining power for short time intervals followed by idle periods. During the idle periods, also called the *relaxation* time, the battery can partially recover the charge lost while delivering the current impulse; this phenomenon is called *recovery effect*.

In this paper, we develop a model for battery behavior that captures the dynamics of the recovery effect and studies the actual gain derived under stochastic pulsed discharge induced by different discharge demand processes. Then, the discharge process is “tailored” through a shaping technique to maximize the energy efficiency of the battery. Using smart battery packages [14], the state of charge of the battery can be monitored. Whenever the battery state of charge drops to a certain threshold, we let the battery rest by interrupting the discharge process at the terminal user. The proposed solution forces a low rate pulsed discharge and guarantees that the battery has chance to recover; in this way, the battery performance is dramatically enhanced. We point out that the approach presented in this paper can apply to any kind of discharge process that takes place in portable wireless devices, provided discharge demand is delay tolerant. An example of possible application is best-effort data transmissions; indeed, the bursty nature of many data traffic sources suggests that data transmissions may provide natural opportunities to exploit the battery recovery effect.

The remainder of the paper is organized as follows. Section II discusses the most relevant characteristics of the battery behavior; Section III presents an analytical model of the battery performance under pulsed current discharge and shows some results; Section IV presents the battery performance when a shaping technique is applied to the discharge process; and, finally, Section V concludes the paper and identifies further topics of research.

## II. BEHAVIOR OF ELECTROCHEMICAL CELLS

Batteries store chemical energy and deliver electrical energy through an electrochemical conversion process. A battery con-

Manuscript received August 1, 1999; revised March 1, 2001. This work was supported by the National Science Foundation under Grant CCR 9714651.

C.-F. Chiasserini is with the Dipartimento di Elettronica, Politecnico di Torino, 10129 Torino, Italy (e-mail: chiasserini@polito.it).

R. R. Rao is with the Center for Wireless Communications, University of California, San Diego, La Jolla, CA 92093-0407 USA (e-mail: rao@cw.cw.ucsd.edu).

Publisher Item Identifier S 0733-8716(01)04998-8.

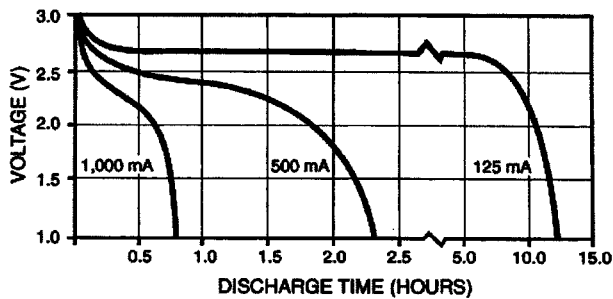


Fig. 1. Discharge behavior of a lithium-ion cell with  $V_{OC} = 3$  V and  $V_{cut} = 1.0$  V.

sists of one or more *cells*, organized in an array. Each cell consists of an anode, a cathode, and the electrolyte that separates the two electrodes and allows the transfer of electrons as ions between them [8]. Chemical material that originates chemical reactions within the cell is called *active material*.

The ideal electrochemical cell should be extremely light, able to provide an infinite amount of energy, and to handle all the desired levels of power. In practice, the energy that can be obtained from a cell is fundamentally limited by the quantity of active material contained in the cell. Therefore, the lighter the cell, the smaller its capacity. In fact, there is a measure of the capacity of a cell, named theoretical capacity, that is a function only of the type and mass of the electrodes and electrolytes. While one cannot hope to exceed this capacity, the challenge in cell design is to come close to this capacity. In practice, the delivered energy greatly depends on the intensity of the discharge current, the power level drained from the cell, and whether the discharge is constant or pulsed.

#### A. Notations and Definitions

A *cell* is characterized by three voltage values: 1) the initial open-circuit voltage ( $V_{OC}$ ), i.e., the initial value of voltage of the fully charged cell under no-load conditions; 2) the operating voltage of the cell under load conditions expressed as volt and denoted by  $V$ ; and 3) the cutoff voltage at which the cell is considered discharged, denoted by  $V_{cut}$  (namely 80% of the  $V_{OC}$ ). Two parameters are used to represent the cell capacity: the *theoretical* and the *nominal* capacity. The former is based on the amount of active material contained in the cell and is expressed in terms of ampere-hours. The latter represents the ampere-hours obtained from a cell when it is discharged at a specific constant current to a specific cutoff voltage.

Finally, to measure the cell discharge performance, the following parameters are considered. *Discharge time* ( $t_l$ ) is expressed as seconds elapsed until a fully charged cell reaches the  $V_{cut}$  voltage and has to be replaced or recharged. *Discharge current* (*current density*) ( $I$ ) is expressed as amperes (amperes per  $\text{cm}^2$ ) drained from a cell. *Specific power* (*energy*) is the power (energy) expressed as watt (watt-hour) per kilogram delivered by a fully charged cell at a specified current of discharge. Likewise, *specific capacity*, expressed as ampere-hours per kilogram, can be defined.

To clarify the above definitions, Fig. 1 from [15] shows the constant current discharge behavior of a lithium-ion cell with

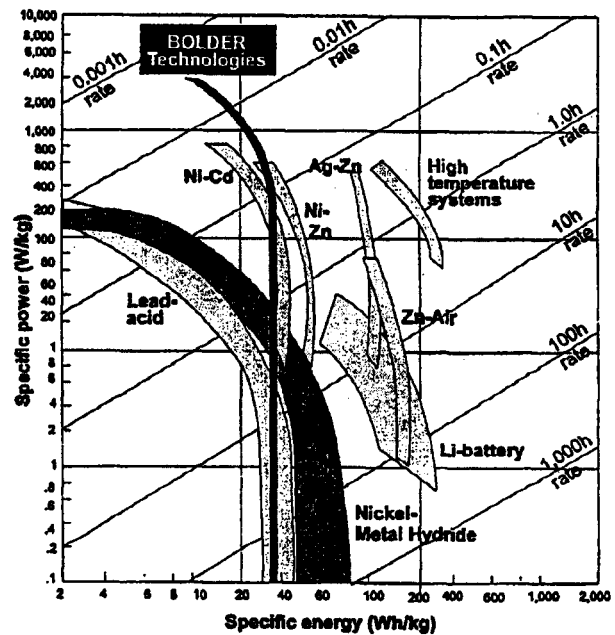


Fig. 2. Ragone plots for various battery chemistries.

$V_{OC} = 3$  V and  $V_{cut} = 1.0$  V. The three curves in the plot correspond to different values of the discharge current.

#### B. Capacity of Electrochemical Cells

The electrical current obtained from a cell results from electrochemical reactions occurring at the electrode-electrolyte interface [8], [13], [16]. At zero current, the concentration of the active material in the cell is uniform. As the discharge current increases, the active material is consumed at the electrode-electrolyte interface by electrochemical reactions, and replaced by new active material that moves from the electrolyte solution to the electrode through *diffusion*. As the intensity of the current is increased, the deviation of the concentration from the average becomes more significant and the state of charge as well as the cell voltage decrease. Beyond a threshold value, the so-called *limiting* current, the diffusion phenomena is unable to compensate for the depletion of active material and the cell voltage drops below the usable value even though the theoretical capacity of the cell may not have been exhausted.

The relationship between the discharge time  $t_l$  and the discharge current  $I$  (assuming constant discharge) is given by Peukert's formula [8]

$$t_l = KI^{-h} \quad (1)$$

where  $K$  and  $h$  are constants depending on the cell design and battery chemistry. (Typical values of  $K$  and  $h$  in commercial secondary cells are in the range 10–100 and 1.0–1.5, respectively.) With  $V_a$ , denoting the average value of the cell voltage during the discharge, the specific energy of the cell  $E$  is given by

$$E = V_a \cdot I \cdot t_l = V_a \cdot KI^{1-h}. \quad (2)$$

(We notice that, by considering the average value of the cell voltage during discharge, the specific energy is proportional to the specific capacity of the cell.)

TABLE I  
SUMMARY OF EXPERIMENTAL RESULTS ON PULSED DISCHARGE OF ELECTROCHEMICAL CELLS

Cell type	Experiment	Result
Lead-acid	Current pulses 3ms long followed by a idle time of 22ms [11].	Drained current decreased from 12A/cm <sup>2</sup> (1st pulse) to 7A/cm <sup>2</sup> (6th pulse); the initial $V_{OC}$ was recovered during the first 4 pulses only.
Lithium-ion 600W/kg initial spec. power	Const. discharge to 80% of $V_{OC}$ , then a current pulse 30s long was drained [10].	Spec. power obtained from the pulse was 320 W/kg for no idle time after const. discharge, 490W/kg for a idle period 20min. long.
Sony Li-ion 1Ah nominal capacity	Const. discharge at 1.9A for 16ms followed by a idle time 20min. long [10].	At the end of idle time, the cell voltage was again very close to $V_{OC}$ .
TMF (Thin Metal Film)	Discharge at const. current equal to 100A and at 100A pulses 1s long and followed by a idle time 1s long [13].	Capacity obtained from const. discharge was 0.44Ah, from pulsed discharge 0.5Ah (13.6% of improvement). Even under pulsed discharge, delivered capacity was only 41.7% of the theoretical capacity.
Li-polymer	Current pulses 10ms long followed by a 50ms idle time [20].	Up to 50mA/cm <sup>2</sup> (about 14 times the typical const. discharge current) was obtained.

Equations (1) and (2) highlight the inverse relationship between discharge time and specific energy on the one hand and discharge current on the other. The relationship between specific energy and specific power of a number of different batteries is displayed in the so-called Ragone plot reproduced from [11] as Fig. 2. The fact that the curves lean to the left shows that a high specific energy can be obtained only if the discharge is at low power levels. Even if one settles for a low discharge current (i.e., a low specific power), the capacity delivered by a battery under constant discharge is typically only 10%–30% of the theoretical value. Although improvements in battery technology are being made, they tend to lag behind the demand. We are, therefore, led to ask if, for a given battery chemistry, there is a way to improve the yield. Perhaps the answer lies in the fact that in some applications (such as data transmissions) one might expect the discharge to be bursty. How does bursty discharge effect cell capacity?

### C. Pulsed Discharge

Some of the adverse consequences of constant current discharge can indeed be overcome when the discharge is pulsed. If a cell is allowed to relax long enough after delivering a pulse, the concentration gradient of the active material decreases and charge recovery takes place at the electrode. As already mentioned, this recovery effect is due to the diffusion process that compensates for the depletion of active material.

Several findings [8], [10]–[13], [17]–[20] quantify the advantages that result from a pulsed current discharge mode. Table I reports experimental results obtained by using different cell technologies. We point out that the discharge time in these experiments are much longer than the typical timing used in radio communication systems; however, these results clearly prove that, for a fixed power level, the delivered specific energy can be increased by using a pulsed discharge instead of a constant discharge. By using a pulsed discharge, a higher specific power

can be drained from the cell for a constant delivered specific energy (e.g., see the experiment on Li-polymer cells).

Also, the experiment on lead-acid cells [11] reported in Table I shows that the cell ability to recover charge during idle time decreases as the cell discharges. This indicates that different stages of the discharge process, so-called *discharge phases*, can be identified, and, depending on the cell discharge phase, the recovery period should be properly controlled by modulating the discharge profile in order to increase the delivered specific energy. A similar observation can be made about the experiment on thin metal film (TMF) cells [13], [17].

It is important to notice that the benefits of pulsed discharge continue to hold if the discharge is composed of pulses superimposed on a constant background current [12], [21], [22]. Such discharge patterns are likely in communication devices where the baseband and RF parts need a constant supply, but load changes occur whenever the system passes from the idle to the active state or the radio transceiver switches from receiver to transmit mode. For instance, in the case of a WLAN card, the current consumed in transmit mode is 1.5 times greater than the current consumed in receiver mode and 30 times higher than the current consumed in doze mode [2]. Experimental results reported in [21] and [22] prove that, even if a constant background current is drained, during the idle periods between successive pulses the cell is able to recover charge and its voltage arises to the value of operating voltage associated to the constant background current discharge. Thus, an improvement in delivered specific energy is still obtained; clearly, the greater the difference between background current and pulsed current, the greater the improvement.

These findings suggest that, in applications that can tolerate a bursty power supply, there might be an opportunity to enhance battery efficiency by controlling the time instants of discharge. In order to explore these possibilities systematically, it is imperative that we develop a reasonable model for battery behavior.

### III. MODELS FOR STOCHASTIC DISCHARGE

In this section, we examine ways to model battery behavior mathematically in terms of parameters that can be related to physical characteristics of the electrochemical cell.

Electrochemical models that give a detailed representation of the electrochemical phenomena taking place within the cell can be found in the literature [12], [23]. They are based on partial differential equation systems, whose complexity prevents the use of electrochemical models for communications system modeling and protocol design. Here, the goal is not to be overly specific, but to capture enough details in a tractable manner and use a stochastic model to develop a broad category of protocols for energy efficient communications. We point out that none of the models for cell discharge proposed in the literature apply in a stochastic setting [9], [10], [12], [16], [23].

Let us consider a single cell and track the stochastic evolution of the cell from the fully charged to the completely discharged state. Models for arrays of cells can be developed from this simple cell. In the following analysis, the background current (see Section II-C) is neglected for the sake of simplicity. Indeed, since the benefits of pulsed discharge remain unchanged in the presence of background current, the following analysis can be still applied by simply scaling down the available cell capacity by a factor corresponding to the required background current [12], [21].

We assume that the time scale is divided in time slot intervals with unit duration, and we define the basic amount of capacity that is drained from a cell as one *charge unit*. Each fully charged cell is assumed to have a theoretical capacity equal to  $T$  charge units, and a nominal capacity equal to  $N$  charge units. The theoretical capacity  $T$  is a function of the mass and nature of the electrodes and the electrolyte and as such is unaffected by discharge profiles. The nominal capacity  $N$  is much less than  $T$  for all cell technologies and represents the charge that could be extracted using a constant discharge profile. Our ultimate goal is to extract an amount of charge that exceeds  $N$  through pulsed discharge.

Discharges occur at stochastic instants determined by the discharge pattern and recovery may occur whenever there is no discharge. In particular, in each time slot if a discharge occurs, as many charge units as required by the discharge pattern are lost; otherwise the battery may recover one charge unit or remain in the same state. The amount of charge recovered in one time slot was chosen equal to one charge unit at most to reproduce the cell behavior obtained by using an electrochemical model of a lithium-ion cell [23], [24]. Lithium-ion cells are vastly used in communication systems; however, a similar behavior is expected of other types of cells since the recovery effect dynamics are quite the same. To more accurately model real cell behavior [23]–[25], the recovery effect that takes place when no discharge occurs is modeled stochastically representing the fact that the recovery capability of the cell decreases as the cell is discharged [11], [25] (see Section II-C). The probability to recover one charge unit during an idle slot is modeled as a decreasing exponential function of the state of charge and discharged phase, and the exponential decay coefficient is assumed to take different values as a function of the discharged capacity. Such a

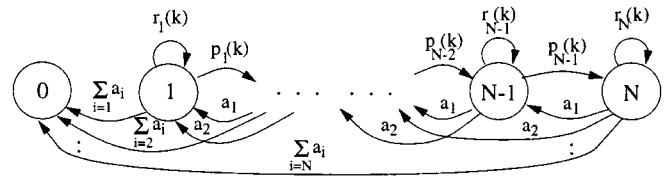


Fig. 3. Graphical representation of the stochastic process modeling the cell behavior.

model was used in [26] in a nonstochastic setting. In [27], we validated the stochastic model by comparing results in terms of the cell's delivered energy with those obtained through the electrochemical model of a lithium-ion cell [23], [24].

#### A. Dynamics of Charge Recovery

The resulting cell behavior is a transient stochastic process that starts from the state of full charge ( $V = V_{OC}$ ), denoted by  $N$ , and terminates when state 0 (corresponding to a complete discharge of the cell) is reached, or the theoretical capacity  $T$  is exhausted. Note that, due to the limited theoretical capacity of the cell, at most  $T$  charge units can be drained.

Let us define  $a_i$  to be the probability that  $i$  discharge requests, each one requiring one charge unit, arrives in one time slot. Thus, in each time slot, the cell has probability  $a_i$  to move from state  $z$  to  $z - i$ , with  $0 < z \leq N$ , where the positions corresponding to  $z - i < 0$  add to the probability to move to 0.

The recovery probability in state  $j$  after  $k$  charge units have been drained is as follows:

$$p_j(k) = \begin{cases} a_0 e^{-(N-j)\alpha_N - \alpha_C(k)}, & j = 1, \dots, N-1 \\ & k = 0, \dots, \Gamma_1 \\ a_0 e^{-(N-j)\alpha_N - \Gamma_c \alpha_C(k)}, & j = 1, \dots, N-1 \\ & \Gamma_c < k \leq \Gamma_{c+1} \\ & c = 1, \dots, c_{\max} - 1 \end{cases} \quad (3)$$

where  $c_{\max}$  is the number of discharge phases that characterize the cell behavior,  $\Gamma_{c_{\max}} = T$ , and  $\alpha_N$  and  $\alpha_C(\cdot)$  depend on the recovery capability of the battery. In particular, a small value of  $\alpha_N$  represents a high cell conductivity (i.e., a high recovery capability), while a large  $\alpha_N$  corresponds to a high internal resistance (i.e., a low recovery capability and, hence, a steep discharge curve for the cell). The value of  $\alpha_C(\cdot)$  is related to the cell voltage drop during the discharge process and, therefore, to the discharge current. We assume that  $\alpha_N$  is a constant, whereas  $\alpha_C(\cdot)$  is a piecewise constant function of the number of charge units already drawn off the cell, that changes value in correspondence with  $\Gamma_c$  ( $c = 1, \dots, c_{\max} - 1$ ).

The probability to remain in the same state of charge is

$$\begin{aligned} r_j(k) &= a_0 - p_j(k) \quad j = 1, \dots, N-1; \quad k = 0, \dots, T \\ r_N(k) &= a_0 \quad k = 0, \dots, T. \end{aligned} \quad (4)$$

Fig. 3 shows a graphical representation of the process. Note that in [28]  $p_j(k)$  and  $r_j(k)$  were assumed to be constant for any  $j$  and  $k$  since it was not considered the dependence on the cell state of charge and discharged capacity.

We want to derive the average number of charge units,  $\bar{m}_p$ , drained during the cell discharge process starting from state  $N$ . We start our analysis considering the process evolution in the generic phase  $c$ . Since in each discharge phase the transition probabilities  $p_j(k)$  and  $r_j(k)$  are constant values, we have

$$\begin{aligned} p_j(k) &= p_j^{(c)}; & r_j(k) &= r_j^{(c)} \\ j &= 1, \dots, N-1; & \Gamma_c &< k \leq \Gamma_{c+1}; \\ c &= 0, \dots, c_{\max} - 1. \end{aligned} \quad (5)$$

We define  $u_{b,e}^{(c)}(h, n)$  as the probability to reach state  $e$  ( $0 \leq e \leq N$ ) in  $n$  steps starting from state  $b$  ( $1 \leq b \leq N$ ) and consuming  $h$  charge units, with  $0 \leq h \leq (\Gamma_{c+1} - \Gamma_c)$ . Referring to Fig. 3, we can write

$$\begin{aligned} u_{N,e}^{(c)}(h, n) &= r_N^{(c)} u_{N,e}^{(c)}(h, n-1) \\ &+ \sum_{i=1}^{\min(h, N-1)} a_i u_{N-i,e}^{(c)}(h-i, n-1) \\ &+ \sum_{i=N}^{\infty} a_i \delta_{e,0} \delta(h-N) \delta(n-1) \\ &+ \delta_{N,e} \delta(h) \delta(n) \quad n \geq 0 \end{aligned} \quad (6)$$

$$\begin{aligned} u_{b,e}^{(c)}(h, n) &= r_b^{(c)} u_{b,e}^{(c)}(h, n-1) + p_b^{(c)} u_{b+1,e}^{(c)}(h, n-1) \\ &+ \sum_{i=1}^{\min(b-1, h)} a_i u_{b-i,e}^{(c)}(h-i, n-1) \\ &+ \sum_{i=b}^{\infty} a_i \delta_{e,0} \delta(h-b) \delta(n-1) \\ &+ \delta_{b,e} \delta(h) \delta(n) \quad 1 < b < N; \quad n \geq 0 \end{aligned} \quad (7)$$

$$\begin{aligned} u_{1,e}^{(c)}(h, n) &= r_1^{(c)} u_{1,e}^{(c)}(h, n-1) + p_1^{(c)} u_{2,e}^{(c)}(h, n-1) \\ &+ \sum_{i=1}^{\infty} a_i \delta_{e,0} \delta(h-1) \delta(n-1) \\ &+ \delta_{1,e} \delta(h) \delta(n) \quad n \geq 0 \end{aligned} \quad (8)$$

where

$$\delta_{x,y} = \begin{cases} 1, & \text{if } x = y \\ 0, & \text{else} \end{cases} \quad (9)$$

and

$$\delta(x) = \begin{cases} 1, & \text{if } x = 0 \\ 0, & \text{else.} \end{cases} \quad (10)$$

By using the method of generating functions [29], we compute the  $Z$  transform of (6)–(8) with respect to  $n$

$$\begin{aligned} U_{N,e}^{(c)}(h, z) &= r_N^{(c)} z U_{N,e}^{(c)}(h, z) \\ &+ \sum_{i=1}^{\min(N-1, h)} a_i z U_{N-i,e}^{(c)}(h-i, z) \\ &+ \sum_{i=N}^{\infty} a_i \delta_{e,0} \delta(h-N) z + \delta_{N,e} \delta(h) \end{aligned} \quad (11)$$

$$\begin{aligned} U_{b,e}^{(c)}(h, z) &= r_b^{(c)} z U_{b,e}^{(c)}(h, z) + p_b^{(c)} z U_{b+1,e}^{(c)}(h, z) \\ &+ \sum_{i=1}^{\min(b-1, h)} a_i z U_{b-i,e}^{(c)}(h-i, z) \\ &+ \sum_{i=b}^{\infty} a_i \delta_{e,0} \delta(h-b) z + \delta_{b,e} \delta(h) \end{aligned} \quad 1 < b < N \quad (12)$$

$$\begin{aligned} U_{1,e}^{(c)}(h, z) &= r_1^{(c)} z U_{1,e}^{(c)}(h, z) + p_1^{(c)}(h) z U_{2,e}^{(c)}(h, z) \\ &+ \sum_{i=1}^{\infty} a_i \delta_{e,0} \delta(h-1) z + \delta_{1,e} \delta(h) \end{aligned} \quad (13)$$

and we evaluate (11)–(13) for  $z = 1$ . We can use the recursion (11)–(13) to compute the values  $U_{b,e}^{(c)}(h, 1)$  ( $1 \leq b \leq N$ ), so that the process evolution in phase  $c$  ( $c = 0, \dots, c_{\max} - 1$ ) is derived.

However, since multiple charge units may be required in a time slot, we have to consider the event that more than  $(\Gamma_{c+1} - \Gamma_c)$  charge units are consumed while being in discharge phase  $c$ . By assuming that from the generic phase  $c$  the cell cannot move beyond phase  $c+1$  in one step, the probability of this event is equal to the probability to consume  $l$  charge units without leaving phase  $c$ , times the probability to drain  $h-l$  charge units in a time slot such that phase  $c+1$  is entered.

We denote by  $v_{b,e}(j)$  the probability that a discharge request makes the cell pass from a phase to the next one while moving from state  $b$  to state  $e$  and consuming  $j$  charge units. Then

$$\begin{aligned} v_{b,e}(j) &= \\ &\begin{cases} a_j \delta(j - (b - e)) + \sum_{i=j+1}^{\infty} a_i \delta(j - b) \delta_{e,0}, & \text{if } b > e \\ 0, & \text{else.} \end{cases} \end{aligned} \quad (14)$$

Note that  $v_{b,e}(j)$  does not depend on the discharge phase.

At this point, the cell behavior can be tracked through the different phases of the discharge process. We define  $w_{b,e}^{(c)}(h, k)$  as the probability to move from state  $b$  to state  $e$  while being in phase  $c$ , consuming  $h$  charge units ( $0 \leq h \leq T$ ), and conditioned at having already transmitted  $k$  charge units. We have

$$\begin{aligned} w_{b,e}^{(c)}(h, k) &= \\ &\begin{cases} U_{b,e}^{(c)}(h, 1) h \leq \Gamma_{c+1} - k \\ \sum_{l=0}^{\Gamma_{c+1} - k - 1} \sum_{s=1}^N U_{b,s}^{(c)}(l, 1) v_{s,e}(h-l) & h > \Gamma_{c+1} - k. \end{cases} \end{aligned} \quad (15)$$

The average number of charge units drained from the cell during the discharge process is computed considering that the following events may occur: 1) the discharge process terminates in state 0 in phase  $c$  ( $c = 0, \dots, c_{\max} - 1$ ) after  $h$  charge units have been consumed and 2)  $T$  charge units are drawn off the cell without the cell having reached state 0. For example, for  $c_{\max} = 3$ , we obtain

$$\begin{aligned} \bar{m}_p &= \sum_{h=1}^T h \cdot w_{N,0}^{(0)}(h, 0) + \sum_{k=\Gamma_1}^{\Gamma_2-1} \sum_{e_1=1}^N w_{N,e_1}^{(0)}(k, 0) \\ &\cdot \left\{ \sum_{h=\Gamma_1+1}^T h \cdot w_{e_1,0}^{(1)}(h-k, k) \right. \\ &+ \sum_{i=\Gamma_2}^{\Gamma_3-1} \sum_{e_2=1}^N w_{e_1,e_2}^{(1)}(i-k, k) \\ &\times \left( \sum_{h=\Gamma_2+1}^T h \cdot w_{e_2,0}^{(2)}(h-i, i) + T \right. \\ &\left. \left. \cdot \sum_{e_3=1}^N w_{e_2,e_3}^{(2)}(T-i, i) \right) \right\}. \end{aligned} \quad (16)$$

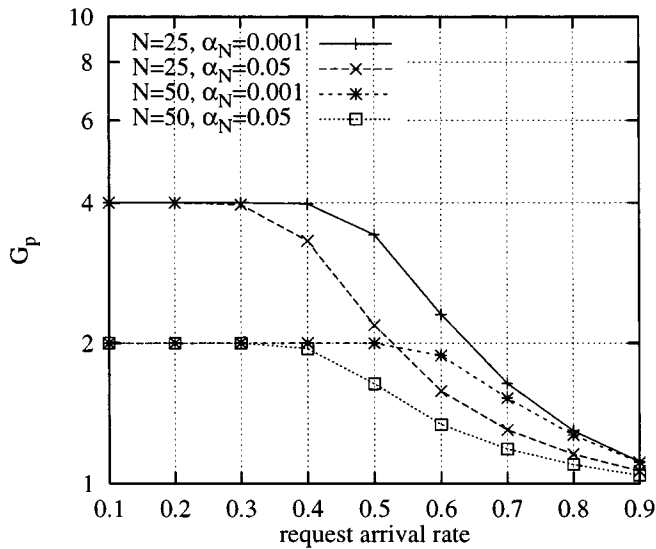


Fig. 4.  $G$  behavior in the case of a Bernoulli-driven discharge demand.  $T = 100$ ,  $N$  and  $\alpha_N$  varying.

Finally, in the case of constant discharge, we assume that the  $N$  charge units drained from a cell can be fully utilized by accumulating charge in a capacitor whenever it needs. Therefore, a measure of the efficacy of pulsed discharge is the ratio

$$G = \frac{\bar{m}_p}{N}. \quad (17)$$

$G$  can be at most equal to  $T/N$ . Pulsed discharge outperforms the constant current discharge to the extent that  $G$  exceeds 1 and approaches  $T/N$ .

### B. Results

The value of  $G$  can be derived for different discharge demand processes. In the following, the behavior of  $G$  is derived as a function of the *discharge request arrival rate*, i.e., the average number of charge units requested per time slot. We assume that  $c_{\max}$  is equal to 3, while the values of the thresholds  $\Gamma_c$  ( $c = 1, \dots, c_{\max} - 1$ ) and the values taken by  $\alpha_C$  are chosen such that the behavior of the cell state of charge during the discharge process presents a realistic profile.

For a Bernoulli discharge process ( $a_1 = R$  and  $a_0 = 1 - a_1$ ), Fig. 4 shows the relationship between  $G$  and the discharge request arrival rate, for  $T = 100$ , and as  $\alpha_N$  and  $N$  vary. Clearly, in this case, the request arrival rate coincides with the value  $R$ . As expected,  $G$  increases as the recovery capability of the cell increases, i.e.,  $\alpha_N$  decreases. In addition, for a fixed  $\alpha_N$ , higher values of  $G$  are obtained as the gap between  $N$  and  $T$  becomes larger; in fact, in this case the margin of improvement that can be exploited through a pulsed discharge is greater. More interestingly, Fig. 4 shows that for any  $\alpha_N$ , no matter what  $N$  is used,  $G$  approaches its lowest value as the request arrival rate increases and approaches its highest value as the request arrival rate decreases. Indeed, for a low discharge demand, the cell may recover often and an amount of charge units equal to the maximum available cell capacity can be drained.

This finding suggests that the burstiness of the discharge process may be a more significant determinant of the delivered capacity than  $N$ , the initial charge stored in the cell, and  $\alpha_N$ ,

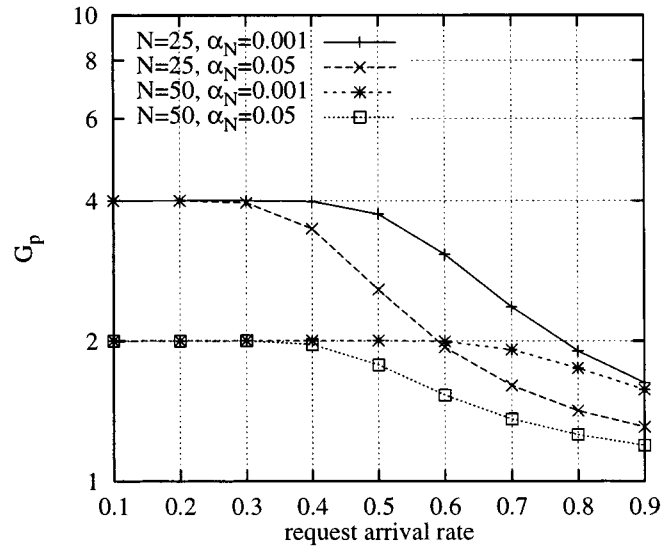


Fig. 5.  $G$  behavior in the case of a discharge demand driven by a truncated Poisson distribution.  $T = 100$ ,  $N$  and  $\alpha_N$  varying.

the recovery capability coefficient. That being so, in Section IV, we study the effect of discharge shaping to maximize  $G$ .

When we deal with a more bursty discharge profile, a truncated Poisson arrival process, the cell performance improves as shown in Fig. 5. Here, we assume that the probability that  $i$  discharge requests arrive in a time slot of unit duration is equal to

$$a_i = \frac{R^i e^{-R} / i!}{\sum_{j=0}^N R^j e^{-R} / j!}, \quad i = 0, \dots, N \quad (18)$$

i.e., the amount of charge units that are drained in a time slot is a random variable that follows a Poisson distribution truncated at the value of nominal capacity  $N$ . In this case, the request arrival rate is equal to

$$\sum_{i=0}^N i \cdot a_i = 1 - \frac{R^N}{N!} \sum_{j=0}^N \frac{j!}{R^j}. \quad (19)$$

## IV. SHAPING THE CELL DISCHARGE

In order to match the discharge profile to the inherent recovery effect of the electrochemical cell, we propose a battery management technique that is similar to the *leaky bucket* algorithm [30]. The objective is to maximize  $G$ , i.e., to increase the ratio of the capacity<sup>1</sup> that can be drawn off a cell to the nominal capacity  $N$ , for any value of  $N$ ,  $\alpha_N$ , and discharge request arrival rate.

### A. Shaping Algorithm

Portable devices normally have a buffer to store service requests [1]. Our idea is to interrupt the discharge process and queue discharge requests whenever the cell state of charge drops to a certain threshold; in this way, the opportunity for charge recovery is significantly increased.

Let  $B$  denote the state of charge chosen as threshold, with  $B$  expressed as charge units, and  $M$  denote the quantity  $N - B$ ,

<sup>1</sup>We recall that an increase in the (specific) capacity drained from a cell corresponds to a roughly equal increase in the (specific) delivered energy (see Section II-B).

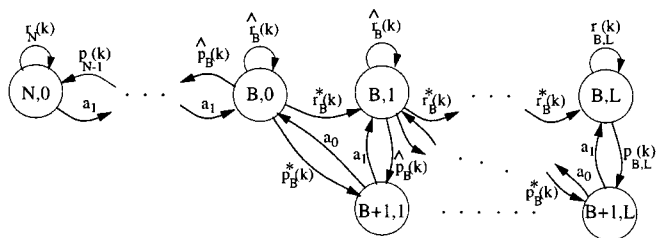


Fig. 6. Graphical representation of the stochastic process modeling the cell behavior when the discharge profile is Bernoulli-driven and the discharge shaping is implemented.

where  $N$  is the cell nominal capacity. As before, we discretize the time scale into time slots with unit duration, we model the discharge demand process as a stochastic arrival process of charge unit requests, and denote by  $a_i$  the probability that  $i$  discharge requests arrive in a time slot. Whenever the cell state of charge drops to state  $B$  after the completion of a discharge request, discharge is stopped and requests arriving at the system are queued in a buffer. We denote the buffer size by  $L$  and assume that  $L$  is large enough to guarantee a loss probability of discharge requests equal to zero. During idle periods, the cell may recover one charge unit per time slot. If the queue is not empty, a discharge request is served as soon as the cell state of charge becomes greater than  $B$ . Thus, whenever there are queued discharge requests, the cell charge can be equal to  $B + 1$  at most. We notice that when the number of charge units requested to accomplish a task exceeds the number of charge units currently available, as many charge units as possible are drawn off as long as threshold  $B$  is reached. The drained charge is temporarily stored in a capacitor until all the necessary charge is obtained.

We consider as state variables the number of charge units available in the cell and the number of queued discharge requests [30]. A graphical representation of the stochastic process modeling the cell discharge is shown in Fig. 6 in the case of a Bernoulli-driven discharge demand. For  $k = 0, \dots, T$ , we have

$$\hat{r}_B(k) = \frac{r_B(k)a_0}{p_B(k) + r_B(k)}; \quad \hat{p}_B(k) = \frac{p_B(k)a_0}{p_B(k) + r_B(k)}$$

$$r_B^*(k) = \frac{r_B(k)a_1}{p_B(k) + r_B(k)}; \quad p_B^*(k) = \frac{p_B(k)a_1}{p_B(k) + r_B(k)}$$

$$r_{B,L}(k) = \frac{r_B(k)}{p_B(k) + r_B(k)}; \quad p_{B,L}(k) = \frac{p_B(k)}{p_B(k) + r_B(k)}$$

where  $p_B(k)$  and  $r_B(k)$  are defined as in (3) and (4) for  $j = B$ .

### B. Results

By applying the shaping algorithm to cell discharge, we obtain  $G = T/N$ , i.e., the capacity that can be drained from a cell is equal to the theoretical capacity and the value of  $G$  is maximized. However, it is clear that such an improvement in the delivered cell capacity corresponds to an additional delay in charge supply.

In the following, results are presented in terms of service rate and average delay of the discharge requests that the cell is able to guarantee. In particular, service rate is derived as the ratio of the number of drained charge units to the discharge process duration; while average delay is obtained by considering the

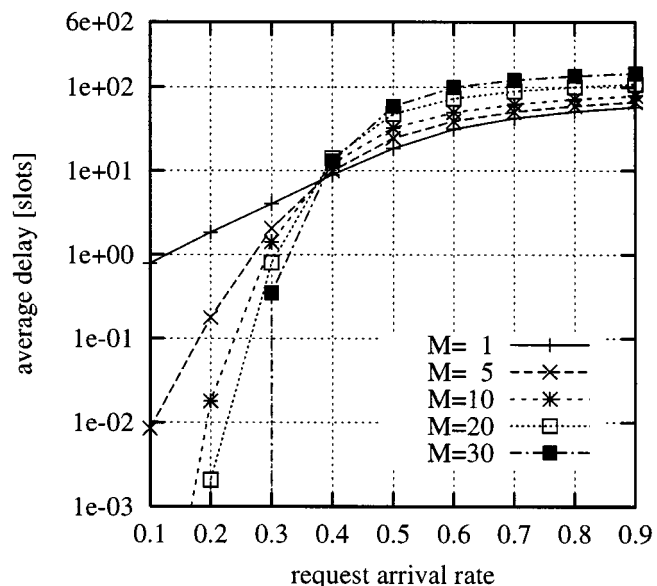
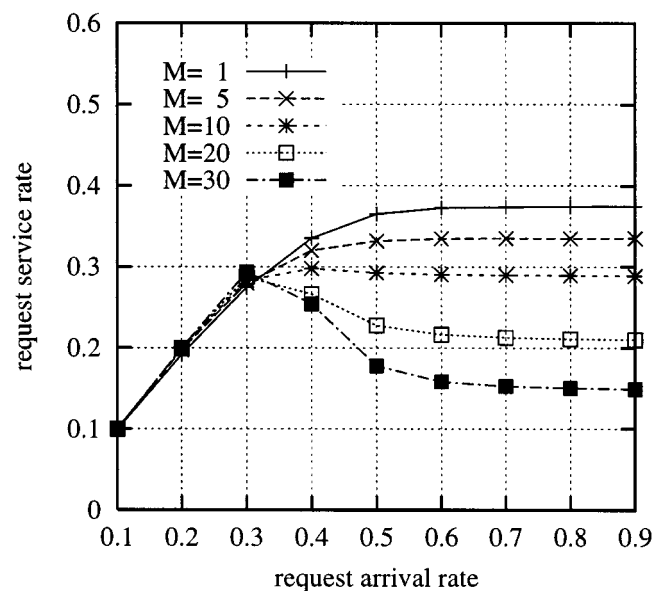


Fig. 7. Bernoulli-driven discharge demand: Cell performance as a function of the discharge request arrival rate for  $T = 100$ ,  $\alpha_N = 0.05$ , and  $M$  varying.

delay from the time instant when a discharge request arrives at the buffer to the time instant when it is served, conditioned to being actually satisfied. Observe that some devices may transit to sleep mode after they have been idle for a certain time. In this case, the time delay associated with a discharge request should include the time the device needs to pass from the sleep to the active state. This delay contribution has not been considered here.

Results are obtained by solving the stochastic process described above via simulation and are presented as functions of the request arrival rate. Plots show that by properly selecting  $M$  or equivalently  $B$ , performance can be optimized as the characteristic parameters of the cell and the discharge profile process change.

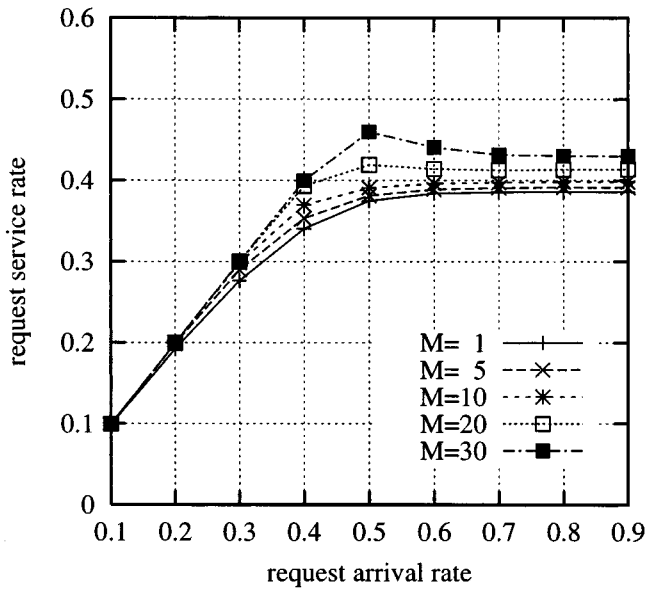


Fig. 8. Bernoulli-driven discharge demand: Cell performance as a function of the discharge request arrival rate for  $T = 100$ ,  $\alpha_N = 0.001$  and  $M$  varying.

Results obtained for a Bernoulli-driven discharge process and  $T = 100$  are presented in Figs. 7 and 8 as  $M$  and  $\alpha_N$  vary. It can be seen that for  $\alpha_N = 0.05$  better results are obtained for low values of  $M$  (i.e., high values of  $B$ ), while for a smaller value of  $\alpha_N$ , performance improves as  $M$  increases (i.e.,  $B$  decreases). This can be explained as follows. For a high value of  $\alpha_N$ , the recovery probability greatly reduces as the cell state of charge decreases; in this case, it is important to prevent the cell state of charge from assuming very low values. Thus, if a small  $M$  is used (i.e., threshold  $B$  is taken close to  $N$ ), better performances are obtained. On the contrary, when  $\alpha_N$  is small, the recovery capability of the cell remains significant even at low values of the state of charge. Then, a large  $M$  is more desirable since it allows for a higher service rate and a smaller average delay of the discharge requests.

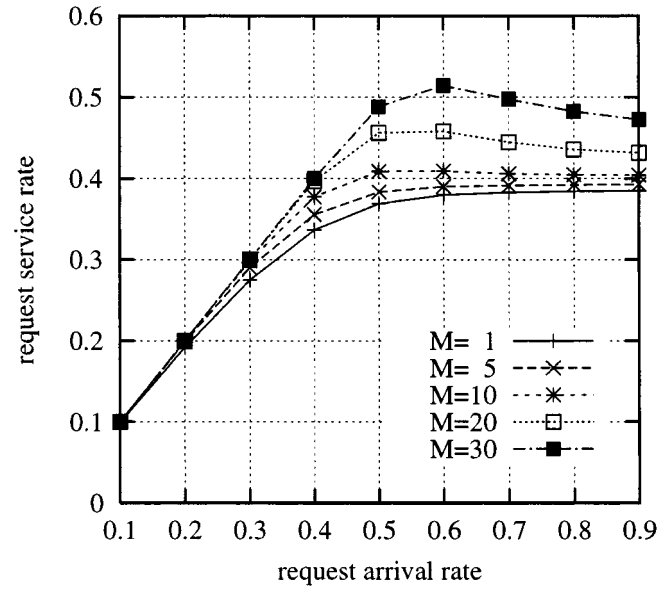


Fig. 9. Discharge demand driven by a truncated Poisson distribution: Cell performance as a function of the discharge request arrival rate for  $T = 100$ ,  $\alpha_N = 0.001$  and  $M$  varying.

From Figs. 7 and 8, it can be seen that for both the values of  $\alpha_N$  and for any value of  $M$ , the average delay increases when high values of the request arrival rate are considered. In fact, the delay introduced between the arrival of a discharge request and the time instant of its service becomes greater. We also notice that, when high values of  $M$  are considered, the service rate decreases as the request arrival rate grows. This is because for a fixed  $N$ , high values of  $M$  correspond to low values of  $B$ , and, therefore, to a lower recovery probability at the threshold state. For high arrival rates, the cell is quickly discharged to threshold state  $B$  in order to satisfy the incoming discharge requests, and the time necessary to recover charge becomes larger. As a consequence, the time needed to drain from the cell a number of charge units equal to the theoretical capacity  $T$  increases. As expected from what we observed before, the degradation of the

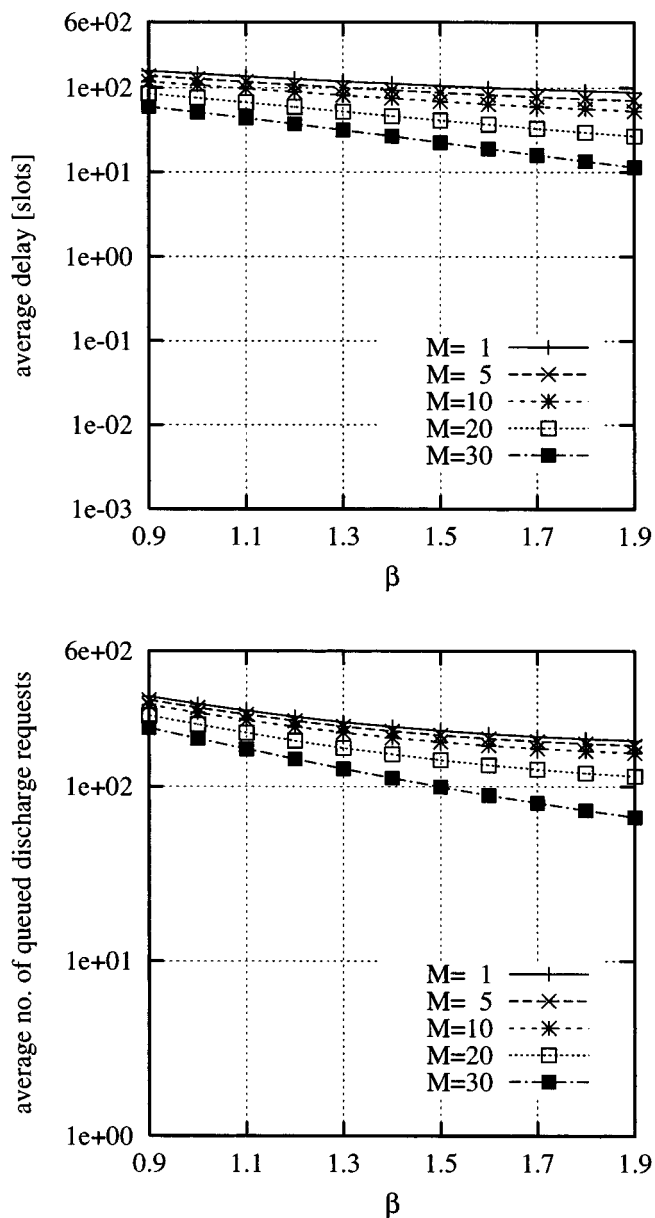


Fig. 10. An ON–OFF source with ON and OFF times Pareto distributed: Cell performance as a function of  $\beta$  and for  $T = 100$ ,  $\alpha_N = 0.001$ , and different values of  $M$ .

service rate is more evident for greater values of  $\alpha_N$  since in this case the reduction of the recovery probability at state  $B$  is more significant.

Similar curves are obtained in the case of a discharge demand process that follows a truncated Poisson distribution as described in Section III-B. Fig. 9 shows results for  $\alpha_N = 0.001$  and  $T$  equal to 100. Results improve as  $M$  increases; however, recall that  $M$  cannot increase as much as desired since it must be  $M < N$ . Comparing Fig. 8 to Fig. 9, it can be seen that for high values of  $M$  (namely: 20, 30) cell performance improves in the case of a truncated Poisson distribution, that is when the discharge demand is more bursty. In fact, for a fixed value of request arrival rate, a greater burstiness allows the cell to benefit of a longer idle time between two successive arrivals and the diffusion mechanism is better exploited.

Finally, we consider an ON–OFF arrival process for the discharge requests, each of them requiring one charge unit. The ON and OFF times are random variables taking values according to a Pareto distribution

$$p(x) = \beta k^\beta x^{-\beta-1} \quad \beta, k > 0; \quad x \geq k. \quad (20)$$

An aggregation of such processes results in a self-similar process if the distribution of the ON and OFF time periods is heavy-tailed, i.e.,  $\beta < 2$  [31]. We take  $k = 1$  and  $\beta$  as a varying parameter between 0.9 and 1.9 [31]. This discharge profile is likely in communication devices when the pulsed discharge process is driven by data transmissions.

In this case, we show the average delay and the number of queued discharge requests as functions of parameter  $\beta$ . Fig. 10 illustrates results for  $T = 100$ ,  $\alpha_N = 0.001$ , and different values of  $M$ . As in the previous cases, the larger the value of  $M$ , the more efficient the system behavior. However, the average delay of discharge requests is higher than for the previous discharge profiles. Indeed, during OFF periods no more than  $N - B$  charge units can be recovered, and during ON periods, it is likely that the cell state of charge drops to state  $B$  much before the next OFF time starts. According to the shaping algorithm, when state  $B$  is reached, discharge must be interrupted and requests must be queued; this causes the degradation observed in the cell performance.

For any of the presented discharge profiles, a higher service rate and smaller average delay can be obtained if a less efficient cell discharge may be acceptable. For the desired gain  $G$ , i.e., the required value of delivered capacity, the shaping algorithm can be applied as described above. Cell performance in terms of service rate and average delay improves as much as the target  $G$  approaches 1. Indeed, the smaller  $G$ , the less the number of charge units that have to be drained from the cell; in this case, discharge phases that correspond to a low recovery capability are never entered. Based on the trade-off between cell discharge efficiency and delay introduced in the discharge process, further shaping techniques can be developed.

## V. CONCLUSION

The paper presented some interesting aspects of the battery behavior that can be exploited to improve battery performances. A model of the single electrochemical cell was developed tracking the recovery effect and the benefits of pulsed discharge relative to constant discharge were shown. Then, we proposed a new battery management technique, which maximizes the energy delivered by a cell at the cost of an additional delay. Results show that performance gains accrue when the parameters of the discharge shaping algorithm are correctly matched to the characteristic parameters of the cell.

Further study is still needed to understand the discharge demand process that is generated by the battery powered devices. Ways to shape the actual discharge demand process should be investigated to better conform to the optimal discharge profile of the cell, while still meeting the constraints on the additional delay that is introduced in the cell discharge.

## REFERENCES

- [1] T. Simunic, L. Benini, P. Glynn, and G. De Micheli, "Dynamic power management for portable systems," presented at the IEEE/ACM MobiCom, Boston, MA, Aug. 2000.
- [2] *IEEE 802.11 WaveLAN PC Card—User's Guide*.
- [3] J.-C. Chen, K. M. Sivalingam, P. Agrawal, and R. Acharya, "Scheduling multimedia services in a low-power MAC for wireless and mobile ATM networks," *IEEE Trans. Multimedia*, vol. 1, pp. 187–201, June 1999.
- [4] N. Bambos and J. M. Rulnick, "Mobile power management for maximum battery life in wireless communication networks," *Proc. IEEE Infocom*, pp. 443–450, Mar. 1996.
- [5] B. Narendran, J. Sienicki, S. Yajnik, and P. Agrawal, "Evaluation of an adaptive power and error control algorithm for wireless systems," *Proc. IEEE Int. Conf. Communications*, pp. 349–355, 1997.
- [6] L. Benini, A. Bogiolo, and G. De Micheli, "A survey of design techniques for system-level dynamic power management," *IEEE Trans. VLSI Syst.*, vol. 8, pp. 299–316, June 2000.
- [7] M. Zorzi and R. R. Rao, "Error control and energy consumption in communications for nomadic computing," *IEEE Trans. Comput.*, vol. 46, pp. 279–289, Mar. 1997.
- [8] *Handbook of Batteries*, 2nd ed., McGraw-Hill, New York, 1995.
- [9] E. J. Podhala and H. Y. Cheh, "Modeling of cylindrical alkaline cells. VI: Variable discharge conditions," *J. Electrochem. Soc.*, vol. 141, no. 1, pp. 28–35, Jan. 1994.
- [10] T. F. Fuller, M. Doyle, and J. S. Newman, "Relaxation phenomena in lithium-ion-insertion cells," *J. Electrochem. Soc.*, vol. 141, no. 4, pp. 982–990, Apr. 1994.
- [11] R. M. LaFollette, "Design and performance of high specific power, pulsed discharge, bipolar lead acid batteries," in *Proc. 10th Annu. Battery Conf. Applications and Advances*, Long Beach, CA, Jan. 1995, pp. 43–47.
- [12] R. M. LaFollette and D. Bennion, "Design fundamentals of high power density, pulsed discharge, lead-acid batteries. II Modeling," *J. Electrochem. Soc.*, vol. 137, no. 12, pp. 3701–3707, Dec. 1990.
- [13] B. Nelson, R. Rinehart, and S. Varley, "Ultrafast pulse discharge and recharge capabilities of thin-metal film battery technology," *Proc. 11th IEEE Int. Pulsed Power Conf.*, pp. 636–641, June 1997.
- [14] Intelligent Batteries [Online]. Available: <http://www.cadex.com/cfm/index>
- [15] Lithium Manganese Dioxide. Performance Characteristics [Online]. Available: <http://www.duracell.com/OEM/index.html>
- [16] M. Doyle and J. Newman, "Analysis of capacity-rate data for lithium batteries using simplified models of the discharge process," *J. Applied Electrochem.*, vol. 27, no. 7, pp. 846–856, July 1997.
- [17] B. Nelson, "TMF ultra-high rate discharge performance," in *Proc. 12th Annu. Battery Conf. Applications and Advances*, Long Beach, CA, Jan. 1997, pp. 139–143.
- [18] P. Calvert *et al.*, "Pyrrole copolymers with enhanced ion diffusion rates for lithium batteries," in *Proc. MRS Symp.*, vol. 496, Dec. 1997, pp. 485–491.
- [19] J. W. Halley and B. Nielsen, "Simulation studies of polymer electrolytes for battery applications," in *Proc. MRS Symp.*, vol. 496, Dec. 1997, pp. 101–107.
- [20] H. S. Choe and K. M. Abraham, "Synthesis and characterization of LiNiO<sub>2</sub> as a cathode material for pulse power batteries," in *Proc. MRS Symp.*, vol. 496, Dec. 1997, pp. 303–308.
- [21] B. Le Pioufle, J. F. Fauvarque, and P. Delalande, "Comportement non linéaire des générateurs électrochimiques associés aux convertisseurs statiques. Détection de l'état de charge," *Eur. Phys. J. Appl. Phys.s*, vol. 2, no. 3, pp. 257–265, June 1998. in French.
- [22] J. S. Newman, *Electrochemical Systems*. Englewood Cliffs, NJ: Prentice-Hall, 1991.
- [23] M. Doyle, T. F. Fuller, and J. S. Newman, "Modeling of galvanostatic charge and discharge of the lithium/polymer/insertion cell," *J. Electrochem. Soc.*, vol. 140, pp. 1526–1533, 1993.
- [24] . *FORTTRAN Programs for Simulation of Electrochemical Systems* [Online]. Available: <http://www.cchem.berkeley.edu/~jsngrp/>
- [25] Make the Right Battery Choice for Portables [Online]. Available: <http://www.tadiranbat.com/howrchg.htm>
- [26] J. Alzieu, H. Smimite, and C. Glaize, "Improvement of intelligent battery controller: State-of-charge indicator and associated functions," *J. Power Source*, vol. 67, no. 1–2, pp. 157–161, July–Aug. 1997.
- [27] C. F. Chiasserini and R. R. Rao, "Energy efficient battery management," *IEEE J. Select. Areas Commun.*, vol. 19, pp. 1235–1245, July 2001.
- [28] ———, "Pulsed battery discharge in communication devices," presented at the IEEE/ACM MobiCom, Seattle, WA, Aug. 1999.
- [29] W. Feller, *An Introduction to Probability Theory and Its Applications*, 3rd ed. New York: Wiley, 1968.
- [30] M. Schwartz, *Broadband Integrated Networks*. Englewood Cliffs, NJ: Prentice-Hall, 1996.
- [31] M. Crovella and A. Bestavros, "Self-similarity in world wide web traffic evidence and possible causes," presented at the ACM Sigmetrics Conf., Philadelphia, PA, May 1996.



**Carla-Fabiana Chiasserini** (S'98–M'00) received the Laurea degree in electrical engineering from University of Florence, Italy, in 1996, and the Ph.D. degree from Politecnico di Torino, Italy, in 1999.

Since 1999, she has been with the Department of Electrical Engineering, Politecnico di Torino, as an Assistant Professor. She was with the Center for Wireless Communications, University of California, San Diego, as a Visiting Researcher in 1999 and 2000. Her research interests include architectures, protocols, and performance analysis of wireless

networks.

**Ramesh R. Rao** (M'85–SM'90) received the B.S. degree with honors in electrical and electronics engineering from the University of Madras, India, in 1980. He received the M.S. and the Ph.D. degrees from the University of Maryland, College Park, MD, in 1982 and 1984, respectively.

Since 1984, he has been with the Department of Electrical and Computer Engineering, University of California, San Diego, where he is currently Professor and Director of the Center for Wireless Communications. His research interests include architectures, protocols, and performance analysis of wireless, wireline and photonic networks for integrated multimedia services.

He served as the Editor of the Information Theory Society Newsletter from 1993 to 1995 and is the founding Web Editor of the Information Theory Society web site. He was elected to the IEEE Information Theory Society Board of Governors in 1997 and in 2000. He is the Editor for Packet Multiple Access of the IEEE TRANSACTIONS ON COMMUNICATIONS and is a member of the Editorial Board of the ACM/Baltzer Wireless Network Journal as well as IEEE NETWORK MAGAZINE. He has guest edited special issues of several ACM and IEEE journals. He regularly serves as a member of the Technical Program Committees of IEEE conferences and as a reviewer for agencies such as the National Science Foundation.